

# Photophysical Properties of a Supramolecular Interlocked Conjugate

Andrew C. Benniston,<sup>\*,†</sup> Morven Davies,<sup>‡</sup> Anthony Harriman,<sup>\*,†</sup> and Craig Sams<sup>†</sup>

Molecular Photonics Laboratory, School of Natural Sciences—Chemistry, Bedson Building, University of Newcastle, Newcastle-upon-Tyne NE1 7RU, United Kingdom, and Chemistry Department, Joseph Black Building, University of Glasgow, Glasgow G12 8QQ, United Kingdom

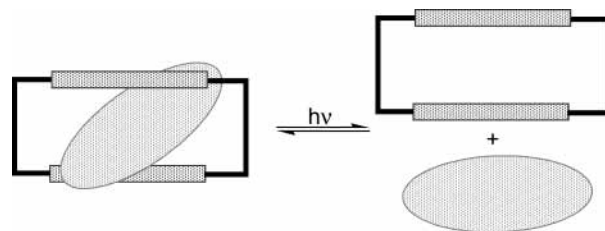
Received: January 19, 2003; In Final Form: March 25, 2003

The binding behavior between a rigid,  $\pi$ -accepting aromatic polycycle (ADIQ·2PF<sub>6</sub>) and an electron-donating crown ether (CE(10)) is reported in acetonitrile solution. In CH<sub>3</sub>CN at low concentration of crown ether, the binding data are consistent with formation of a 1:1 complex in which the ADIQ·2PF<sub>6</sub> residue is partially encapsulated by the crown ether ( $K_1 \approx 500 \text{ dm}^3 \text{ mol}^{-1}$ ). As the mole fraction of crown ether increases, mass spectrometry indicates formation of a molecular aggregate in which two crown ethers are bound to a single ADIQ·2PF<sub>6</sub> entity in the form of a [3]pseudorotaxane. Molecular modeling and NMR spectroscopic studies indicate that the crown ether fits loosely on the end of the polycycle without significant penetration along the molecular axis. Binding causes extinction of fluorescence from the polycycle, allowing estimation of the second binding constant ( $K_2 \approx 400 \text{ dm}^3 \text{ mol}^{-1}$ ), and results in the appearance of a charge-transfer absorption band in the visible region. Illumination into this absorption band promotes formation of an intimate radical ion pair with a time constant of ca. 3 ps. Subsequent charge recombination occurs with a lifetime of ca. 25 ps and results in greatly enhanced population of the triplet excited state localized on the polycycle. There is little or no separation of the radical ion pair into solvated ions.

## 1. Introduction

Numerous elaborate molecular conjugates have been characterized in recent years in an effort to identify components for use in putative molecular-scale devices.<sup>1</sup> A particularly attractive and simple molecular module can be devised by inclusion of a rigid, rodlike guest into a flexible macrocyclic host. Indeed, a variety of such structures are now available,<sup>2</sup> and in certain cases, it has been possible to monitor the assembly and subsequent dissociation of the supramolecular species.<sup>3</sup> These conjugates form by way of diffusional contact between the reactants in solution, and various methods (e.g., photochemical,<sup>4</sup> redox,<sup>5</sup> pH shock,<sup>6</sup> ion binding,<sup>7</sup> isomerization<sup>8</sup>) have been considered by which to perturb the equilibrium distribution. In principle, it should be possible to promote dissociation of the conjugate by selective illumination (Scheme 1), but this has not proved to be effective because of competitive recombination steps.<sup>9</sup> For example, the diquat dication is readily included into a dibenzocrown ether of appropriate dimensions so as to form an intimate charge-transfer complex.<sup>10</sup> Direct illumination into the resultant charge-transfer absorption band causes partial separation of the radical ion pair, but the overall yield of separated ions is rather low. Varying the size and shape of either reactant has some effect on the efficiency of the dissociative process but without leading to major changes in yield.<sup>11</sup> It seems unlikely, on this basis, that further structural modification will lead to the development of prototypes in which illumination causes rapid and selective ejection of the guest from its cavity. The use of sacrificial reagents to drive light-induced dissociation,<sup>12</sup> while being an interesting diversion, remains undesirable since the objective is to design reversible photosystems.

## SCHEME 1: Photoassisted Dissociation of a Cyclophane-Bound Conjugate Pair



Before dismissing this approach for the construction of light-driven molecular machines, it seems appropriate to explore processes other than activated dissociation of the conjugate. To this end, we have examined the photophysical properties of a molecular conjugate formed by including a highly fluorescent guest (ADIQ·2PF<sub>6</sub>) into one or two macrocyclic hosts.<sup>13</sup> Although reminiscent of those systems obtained by inserting *N,N'*-dimethyl-4,4'-bipyridinium (MV<sup>2+</sup>) or *N,N'*-dimethyl-2,7-diazapyrenium dications (DAP<sup>2+</sup>) into the cavity provided by a dibenzocrown ether,<sup>14</sup> this conjugate possesses a quite distinctive electronic energy level system. The key feature of this system is that the triplet excited state localized on the polycyclic guest lies at unusually low energy and is much less energetic than the charge-transfer state formed by intracomplex electron transfer. As such, charge recombination populates the  $\pi,\pi^*$  triplet excited state of the polycycle with much higher probability than found in the absence of complexation. This seems to be an unusual way by which to promote intersystem crossing in organic molecules, although the concept has been well demonstrated for intramolecular charge-transfer states.<sup>15</sup>

## 2. Experimental Section

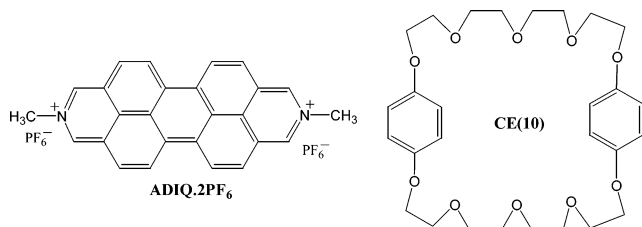
Raw materials were purchased from Aldrich Chemicals Co. and used as received unless stated otherwise. The macrocycle

\* Corresponding author. Telephone: (44) 191 222 8660. Fax: (44) 191 222 8664. E-mail: anthony.harriman@ncl.ac.uk.

<sup>†</sup> University of Newcastle.

<sup>‡</sup> University of Glasgow.

1,4,7,10,17,23,26,28,32-decaoxa[13,13]paracyclophane (CE(10))<sup>16</sup> and the corresponding rigid polycycle *N,N'*-dimethyl-anthra[2,1,9-*def*:6,5,10-*d'e'f'*]diisoquinoline bishexafluorophosphate (ADIQ·2PF<sub>6</sub>)<sup>17</sup> were prepared by literature methods and



purified thoroughly before use. Spectroscopic grade solvents were dried and redistilled under dry nitrogen. <sup>1</sup>H NMR spectra were recorded with a Bruker AM 360 MHz spectrometer using the solvent as internal standard. Absorption and fluorescence spectra were recorded using Hitachi U3310 and Hitachi F4500 spectrophotometers, respectively. Phosphorescence spectra were recorded in the presence of iodomethane (1 mol dm<sup>-3</sup>) using a cryogenic Ge detector in place of the PMT. Mass spectra were recorded using a JEOL The MStation JMS-700 mass spectrometer with *m*-nitrobenzyl alcohol as matrix and operating in positive FAB scan mode. In typical experiments, varying combinations of ADIQ·2PF<sub>6</sub> and CE(10) were prepared in CH<sub>3</sub>CN before being mixed with a small amount of matrix and placed on the probe. Experimental data were sampled after different equilibrium times to ensure consistency.

Binding constants measured by NMR methods were calculated using the EQNMR suite of programs.<sup>18</sup> Fluorescence titrations were made with dilute solutions of ADIQ·2PF<sub>6</sub> (ca. 10<sup>-6</sup> mol dm<sup>-3</sup>) under deoxygenated conditions and in the presence of NH<sub>4</sub>PF<sub>6</sub> (0.1 mol dm<sup>-3</sup>) as background electrolyte. For steady-state experiments, the excitation wavelength was 440 nm and the emission intensity was integrated between 500 and 750 nm for varying concentrations of CE(10). At least 30 different CE(10) concentrations were used for each study. Data analysis was made by nonlinear, least-squares iterative methods, with fitting to appropriate equations using SCIENTIST as a statistical package. The sample cuvette was thermostated at 20 °C, unless stated otherwise, by way of a circulating fluid bath and thermocouple maintained in direct contact with the sample. Time-resolved fluorescence studies were made by the time-correlated, single-photon-counting method using a mode-locked Nd:YAG synchronously pumped, cavity-dumped Styryl-7 dye laser. The excitation wavelength was 370 nm, and fluorescence was isolated from scattered laser light using glass cutoff filters and a high-radiance monochromator. The signal was detected with a cooled microchannel plate photodetector. Data analysis was made after deconvolution of the instrument response function (fwhm = 50 ps).

Transient absorption studies were made with purpose-built nanosecond or subpicosecond laser flash photolysis instruments similar to those described previously.<sup>19</sup> For nanosecond experiments, the sample was adjusted to possess an absorbance of ca. 0.25 at the excitation wavelength and was purged thoroughly with Ar. The sample cell was excited with a 30-ps laser pulse delivered with a frequency-tripled, mode-locked Nd:YAG pumped dye laser operated with Coumarin-440 in ethanol as laser dye. Output from the dye laser, which was centered at 440 nm, was attenuated as necessary with metal screen filters and defocused onto the sample cell. The monitoring beam was provided with a pulsed, high-intensity Xe arc lamp after passing through a collimator and focusing lens. This beam was collected

with a microscope objective, focused onto the entrance slits of a Spex high-radiance monochromator, and detected with a fast-response PMT. The signal was directed to a Textronix transient recorder, averaged, and sent to a fast PC for data analysis. At least 100 individual laser shots were averaged at each wavelength for kinetic measurements. Transient differential absorption spectra were compiled point-by-point, with five laser shots being averaged at each wavelength and collected in random order. The temporal resolution of this instrument was ca. 2 ns, being set by the rise time of the PMT, while the spectral resolution was ca. 3 nm.

For quantitative measurements, the laser intensity was calibrated with zinc *meso*-tetraphenylporphyrin (ZnTPP) in toluene as reference.<sup>20</sup> Thus, the laser intensity was varied over a wide range using crossed polarizers, and the differential absorbance at 470 nm was measured for a deoxygenated solution of ZnTPP adjusted so as to possess an absorbance of 0.25 at the excitation wavelength. The differential absorption coefficient of triplet ZnTPP was taken to be 74 000 dm<sup>3</sup> mol<sup>-1</sup> cm<sup>-1</sup> at 470 nm,<sup>21</sup> and the triplet quantum yield was taken as 0.83.<sup>22</sup> The differential absorption signal at 520 nm for triplet ADIQ·2PF<sub>6</sub> in deoxygenated acetonitrile was recorded over the range of laser intensities where the absorbance for triplet ZnTPP shows a linear dependence on incident intensity. For ADIQ·2PF<sub>6</sub> in acetonitrile, the differential absorption coefficient at 520 nm was found to be 14 100 dm<sup>3</sup> mol<sup>-1</sup> cm<sup>-1</sup> by the complete conversion method.

Improved time resolution was achieved using a mode-locked, frequency-doubled Antares 76S Nd:YAG laser as excitation pump for a Coherent Model 700 pyromethene dual-jet dye laser. A Quantel Model RGA7-10 regenerative amplifier, a Quantel Model PTA-60 dye laser, and a Continuum Model SPA1 autocorrelator were used to produce pulses of around 1 mJ with fwhm of ca. 300 fs. The spectrometer was run at 10 Hz, and the output was split 20:80 to produce excitation and monitoring beams. Output from the dye laser was at 554 nm, and the monitoring pulse was delayed with respect to the excitation pulse using a computerized delay stage. The two beams were directed almost collinearly through the sample cell (path length 5 mm) and detected with a Princeton dual-diode array spectrograph. About 300 individual laser shots were averaged at each delay time, collected in random order, and used to generate kinetic traces by overlaying spectra collected at ca. 40 delay times. Kinetic traces were analyzed by nonlinear, least-squares iteration using global analysis methodology.

Molecular modeling studies were made using the SPARTAN software package<sup>23</sup> run on a fast PC. The structure of ADIQ<sup>2+</sup> was drawn in the molecular mechanics mode and optimized with respect to total energy. A solvent bath of 96 acetonitrile molecules was added, and the two counteranions were positioned randomly around the solute. The structure was subsequently optimized using the parametrized semiempirical AM1 method. One molecule of CE(10) was added to the minimized structure, in a variety of starting positions, and the geometry was again optimized. General convergence of the structure, regardless of starting conformation, was achieved in that the crown ether became attached to the end of the polycycle in a wheel and axle type arrangement. The computations were repeated with two added molecules of CE(10). The final structure appeared as a [3]pseudorotaxane, regardless of starting geometry. In all cases, the counteranions adopted random positions close to the polycycle.

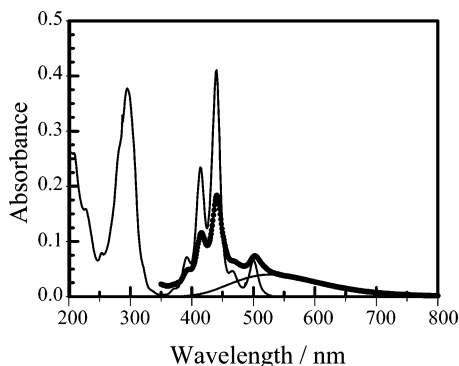


**Figure 1.** Absorption spectrum recorded for a dilute solution of ADIQ·2PF<sub>6</sub> in acetonitrile (solid line) and after addition of excess CE(10) (dotted line). The charge-transfer absorption band appearing at low energy has been fit to a Gaussian-shaped profile that covers the range 400–700 nm.

### 3. Results and Discussion

**a. Formation of a 1:1 Complex.** The absorption spectrum recorded for ADIQ·2PF<sub>6</sub> in acetonitrile consists of four main sets of bands in the visible region centered at 500, 440, 290, and 227 nm that can be assigned to  $\pi,\pi^*$  transitions (Figure 1). Addition of CE(10) to this solution causes a new absorption band to appear as a low-energy tail (Figure 1), while the well-defined  $\pi,\pi^*$  transitions associated with the ADIQ·2PF<sub>6</sub> moiety are somewhat broadened and undergo a slight red shift. There is a significant decrease in absorption associated with some of these  $\pi,\pi^*$  transitions. The absorption tail is highly reminiscent of the charge-transfer absorption bands formed by close association of electron donor–acceptor pairs,<sup>9</sup> although part of the band is obscured by the more intense  $\pi,\pi^*$  transitions. On the basis that this new absorption band is indeed of charge-transfer origin, the profile was fitted to a Gaussian band shape<sup>24</sup> in order to estimate the peak position and molar absorption coefficient (Figure 1). The derived absorption maximum ( $\nu_{\max}$ ) lies at  $18\,950 \pm 200 \text{ cm}^{-1}$ , with the maximum intensity corresponding to a molar absorption coefficient ( $\epsilon_{\max}$ ) of  $800 \pm 40 \text{ dm}^3 \text{ mol}^{-1} \text{ cm}^{-1}$ . As expected for a charge-transfer transition,<sup>25</sup> this band is rather broad and has a half-width of  $2550 \pm 200 \text{ cm}^{-1}$ . Since the spectral perturbations noted for the  $\pi,\pi^*$  transitions are in keeping with  $\pi$ -stacking,<sup>26</sup> it can be surmised that the aromatic groups in CE(10) align to some extent with the planar ADIQ·2PF<sub>6</sub> residue so as to form an intimate charge-transfer complex. It is notable, however, that complexation affects some of the  $\pi,\pi^*$  transitions more than others such that only part of the polycycle might be involved in the binding process.<sup>27</sup>

In such a complex we would expect CE(10) to play the role of electron donor, since the reduction potential for one-electron oxidation ( $E_{\text{OX}}$ ) of the dialkoxybenzene groups is  $1.41 \pm 0.02 \text{ V}$  vs SCE.<sup>11</sup> In contrast, ADIQ·2PF<sub>6</sub> is difficult to oxidize, because of the N-methylated aza groups, but is easily reduced. The reduction potential for one-electron reduction ( $E_{\text{RED}}$ ) of ADIQ·2PF<sub>6</sub> is  $-0.58 \pm 0.02 \text{ V}$  vs SCE.<sup>28</sup> The polycycle undergoes a second reduction step with  $E_{\text{RED}} = -0.71 \pm 0.02 \text{ V}$  vs SCE. These reduction potentials are related to the energy of the charge-transfer absorption band ( $E_{\text{OP}}$ ) as follows:<sup>29</sup>

$$E_{\text{OP}} = E_{\text{OX}} - E_{\text{RED}} + E_{\text{SS}} + \lambda_{\text{T}} \quad (1)$$

where  $\lambda_{\text{T}}$  is the total reorganization energy accompanying charge transfer and  $E_{\text{SS}}$  is a term that corrects for changes in electrostatic interactions between the partners. Assuming the reactants are within orbital contact and remain surrounded by acetonitrile

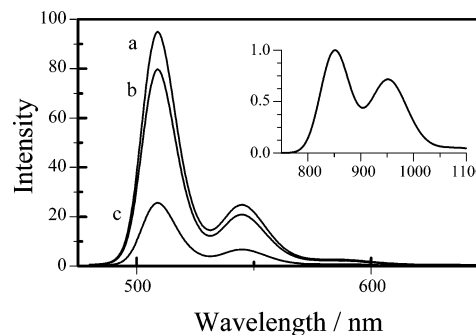


**Figure 2.** Fluorescence spectrum recorded for ADIQ·2PF<sub>6</sub> in dilute acetonitrile solution (a) in the absence and (c) in the presence of CE(10). Curve b shows the effect of added barium perchlorate to solution c. The inset shows the phosphorescence spectrum of ADIQ·2PF<sub>6</sub> recorded in butyronitrile containing iodomethane ( $1 \text{ mol dm}^{-3}$ ) at 77 K.

molecules,  $E_{\text{SS}}$  is calculated to be ca. 0.1 eV.<sup>30</sup> On this basis,  $\lambda_{\text{T}}$  has an approximate value of 0.35 eV. Relative to other charge-transfer complexes,<sup>11</sup> this derived value for  $\lambda_{\text{T}}$  seems to be fairly modest.<sup>31</sup> It can be assigned to structural changes and solvation effects that follow from generation of strong electrostatic repulsion within the emerging radical ion pair. Since the polycycle is rigid, it follows that most of the structural changes will be accommodated by the crown ether.

In dilute acetonitrile solution, ADIQ·2PF<sub>6</sub> fluoresces strongly (Figure 2). The emission maximum is located at 510 nm, but the profile is not a good mirror image of the lowest energy absorption band. The corrected fluorescence excitation spectrum matches very well with the absorption spectrum recorded over the visible and near-UV regions. The fluorescence quantum yield ( $\Phi_{\text{F}}$ ) has a value of  $0.82 \pm 0.05$  in deoxygenated acetonitrile. Fluorescence decay profiles, recorded after laser excitation at 370 nm, are monoexponential at all monitoring wavelengths and correspond to a fluorescence lifetime ( $\tau_{\text{F}}$ ) of  $25.6 \pm 0.2 \text{ ns}$ . The radiative rate constant ( $k_{\text{RAD}} = 4.0 \times 10^7 \text{ s}^{-1}$ ) calculated from the Strickler–Berg expression<sup>32</sup> corresponds closely to that estimated from the experimental values ( $k_{\text{RAD}} = \Phi_{\text{F}}/\tau_{\text{F}} = 3.2 \times 10^7 \text{ s}^{-1}$ ). In the presence of iodomethane ( $1 \text{ mol dm}^{-3}$ ) as heavy-atom perturber,<sup>33</sup> very weak phosphorescence can be detected for ADIQ·2PF<sub>6</sub> in a butyronitrile glass at 77 K (Figure 2). The phosphorescence 0,0 transition is located at ca. 850 nm.

Following excitation of ADIQ·2PF<sub>6</sub> with a 30-ps laser pulse at 440 nm, the corresponding triplet excited state can be observed (Figure 3a). This latter species, which shows an absorption maximum at 520 nm, decays with a first-order rate constant of  $(2.1 \pm 0.1) \times 10^3 \text{ s}^{-1}$  in deoxygenated acetonitrile solution and is formed with a quantum yield of  $0.07 \pm 0.02$  (Figure 3b). At higher laser intensities, the triplet state undergoes bimolecular annihilation to reform the excited singlet state and thereby produce a crop of delayed fluorescence. The singlet state excitation energy ( $E_{\text{S}}$ ), measured at the intersection of normalized absorption and fluorescence spectra, is 2.46 eV, while the triplet state energy ( $E_{\text{T}}$ ), measured from low-temperature phosphorescence spectra, is 1.46 eV. It is notable that these spectroscopic studies place the energy of the charge-transfer state ( $E_{\text{OP}} = 2.34 \text{ eV}$ ) between those of the  $\pi,\pi^*$  excited singlet and triplet states localized on ADIQ·2PF<sub>6</sub>.

Addition of low concentrations ( $< 1 \text{ mmol dm}^{-3}$ ) of CE(10) causes a marked decrease in fluorescence from ADIQ·2PF<sub>6</sub> in acetonitrile solution (Figure 2). There is no obvious change in the fluorescence profile, but there is a slight decrease in the fluorescence lifetime as measured by time-correlated, single-photon counting. Whereas the reduction in fluorescence lifetime

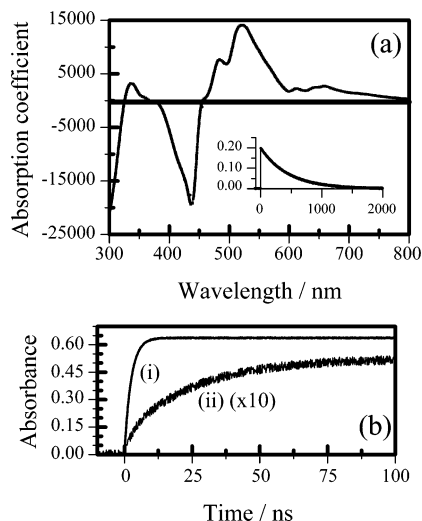


**Figure 3.** (a) Differential absorption spectrum recorded 100 ns after the laser pulse for the triplet excited state of ADIQ·2PF<sub>6</sub> in deoxygenated acetonitrile. The insert shows the decay profile ( $\Delta$ Abs vs time in  $\mu$ s) measured at 520 nm. (b) Growth of the signal at 520 nm following excitation with a 30-ps laser pulse at 440 nm as recorded (i) in the presence and (ii) in the absence of CE(10). Note that trace ii is shown at 10-fold expansion for clarity of presentation.

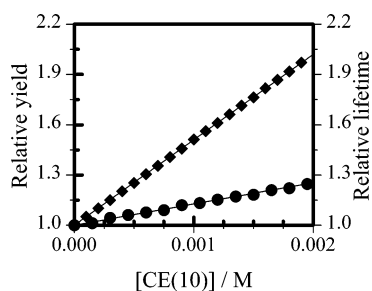


**Figure 4.** Effect of added CE(10) on relative fluorescence quantum yield ( $\blacklozenge$ ) and on relative fluorescence lifetime ( $\bullet$ ) measured at room temperature in deoxygenated acetonitrile.

follows Stern–Volmer kinetics, corresponding to a bimolecular quenching rate constant ( $k_Q$ ) of  $(5 \pm 1) \times 10^9 \text{ dm}^3 \text{ mol}^{-1} \text{ s}^{-1}$ , the attenuation in fluorescence yield is far greater than that expected for diffusion-controlled quenching (Figure 4). On this basis, we assume that fluorescence quenching contains contributions from both dynamic and static processes.<sup>34</sup> The dynamic component corresponds to diffusional quenching of free ADIQ·2PF<sub>6</sub> by CE(10). The static part, which is the dominant process, can be considered in terms of the formation of a 1:1 complex. The steady-state fluorescence data fits reasonably well to a binding constant ( $K_1$ ) of  $500 \pm 100 \text{ dm}^3 \text{ mol}^{-1}$ , provided the concentration of CE(10) is kept modest and that it is assumed the resultant complex does not fluoresce. Support for the latter assumption arises from the time-correlated, single-photon-counting studies which indicate that the complex must possess an excited singlet state lifetime less than ca. 30 ps.

In separate studies it was found that CE(10) does not quench the triplet excited state of ADIQ·2PF<sub>6</sub>. Thus, addition of CE(10) has no observable effect on the triplet lifetime of ADIQ·2PF<sub>6</sub> in deoxygenated acetonitrile at room temperature. On the basis of these studies, the bimolecular rate constant for quenching the ADIQ·2PF<sub>6</sub> triplet must be  $<10^4 \text{ dm}^3 \text{ mol}^{-1} \text{ s}^{-1}$ . Such a finding seems consistent with the low triplet energy associated with the polycycle since electron transfer from the triplet excited state to CE(10) is thermodynamically unfavorable ( $\Delta G^\circ \approx +0.5 \text{ eV}$ ).

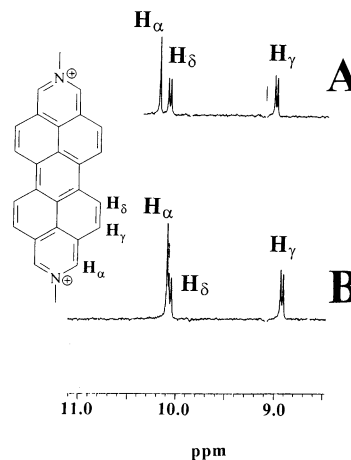


**Figure 5.** Aromatic region of  $^1\text{H}$  NMR spectrum recorded in  $\text{CD}_3\text{CN}$  of (a) ADIQ·2PF<sub>6</sub> and (b) ADIQ·2PF<sub>6</sub> plus 2 equiv of CE(10).

To better characterize the complex, additional studies were undertaken at modest concentrations (i.e.,  $<1 \text{ mmol dm}^{-3}$ ) of crown ether. Thus, in acetonitrile at 20 °C the standard free energy change associated with formation of the complex ( $\Delta G^\circ$ ) has a value of  $-15.1 \text{ kJ mol}^{-1}$ . By measuring the binding constant over a modest temperature range, the corresponding enthalpy ( $\Delta H^\circ$ ) and entropy ( $\Delta S^\circ$ ) changes accompanying complex formation were found to be  $-5.9 \text{ kJ mol}^{-1}$  and  $+31.4 \text{ J K}^{-1} \text{ mol}^{-1}$ , respectively. The positive entropic driving force indicates that complexation involves inclusion of ADIQ·2PF<sub>6</sub> inside the cavity of the crown ether since this would release bound solvent molecules into the bulk solution. Further support for formation of an inclusion complex comes from the observation that the binding constant follows a linear dependence on Gutmann's solvent donor number for a series of aprotic solvents.<sup>3</sup> This effect suggests that the solvent has a strong affinity for the ADIQ<sup>2+</sup> unit, presumably due to ion–dipole interactions at the N-methylated aza part of the molecule.

As outlined above, titration of a dilute solution of ADIQ·2PF<sub>6</sub> in acetonitrile with CE(10) causes loss of the structured fluorescence associated with the electron-affinic polycycle (Figure 2). However, fluorescence is restored upon addition of excess barium perchlorate (Figure 2) due to competitive complexation of  $\text{Ba}^{2+}$  with CE(10).<sup>36</sup> The differential binding constant ( $\Delta K$ ) was calculated by least-squares fitting of the fluorescence data to be  $310 \pm 25$ . This type of fluorescence on/off signal switching has attracted considerable interest over the past few years, especially in the area of nanoscale molecular devices.<sup>37</sup> Practical use of ADIQ<sup>2+</sup> for such systems is hampered, however, by its high fluorescence quantum yield and low binding affinity toward CE(10), which makes complete removal of the fluorescence signal essentially impossible.

Supportive evidence for associative binding between ADIQ·2PF<sub>6</sub> and CE(10) was obtained by high-field  $^1\text{H}$  NMR experiments.<sup>38</sup> Illustrated in Figure 5 are typical spectra of the aromatic region recorded before and after addition of 2 equiv of CE(10) to a solution of ADIQ·2PF<sub>6</sub> in  $\text{CD}_3\text{CN}$ . Two of the aromatic resonances are shifted upfield to differing extents [ $\text{H}_\alpha = -0.35 \text{ ppm}$ ,  $\text{H}_\gamma = -0.28 \text{ ppm}$ ], as is the methyl signal ( $\Delta\delta = -0.05 \text{ ppm}$ ). Such behavior is indicative of the formation of an intimate  $\pi, \pi^*$  stack.<sup>39</sup> It is notable that the  $\text{H}_\delta$  resonance is basically unaffected by the presence of CE(10). Based on these results, it can be concluded that the CE(10) moiety is located at the end of the ADIQ<sup>2+</sup> cation, and does not penetrate onto the central portion of the polycycle. Analysis of the peak shifts using the EQNMR program and assuming 1:1 complexation gives an

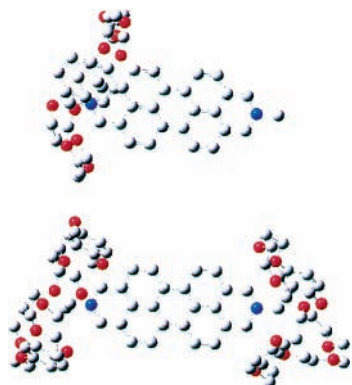


**Figure 6.** Ball-and-stick representations of the optimized structures for the 1:1 complex (upper panel) and 2:1 complex (lower panel) formed between CE(10) and ADIQ•2PF<sub>6</sub>.

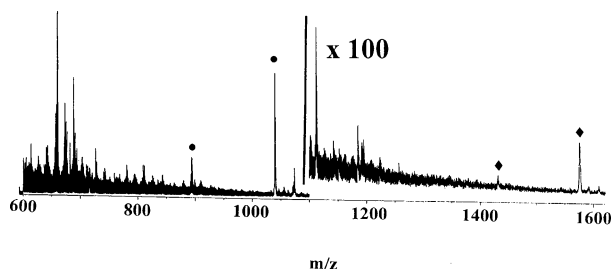


**Figure 7.** Fast atom bombardment mass spectrum recorded for a *m*-nitrobenzyl alcohol matrix sample of the CT complex at a CE(10):ADIQ•2PF<sub>6</sub> ratio of 2:1. The molecular ions for a 1:1 complex are marked (●). Insert shows expanded region of the spectrum, and molecular ions corresponding to a 2:1 complex are marked (◆).

approximate binding constant of  $360 \pm 50 \text{ dm}^3 \text{ mol}^{-1}$ , which is in reasonable agreement with the value derived from fluorescence quenching.

Computer molecular modeling studies were made with the reactants dispersed in a matrix of 96 acetonitrile molecules and starting with a fixed stoichiometry of 1:1. Various starting conformations were tried, and the initial positions of the two PF<sub>6</sub><sup>-</sup> anions were also varied. Illustrated in Figure 6 is the energy-minimized molecular structure of the 1:1 complex, which fully corroborates the NMR finding that binding of the CE(10) subunit occurs only at one end of the ADIQ<sup>2+</sup> molecule. There is a dominant charge-dipole interaction between the N-methylated aza group and five of the oxygen atoms of the polycycle; the other five oxygens appear not to be involved in the binding process at any given instant. Evidently there must exist a “nest” of structures containing only five bound oxygen atoms since rotation of the polycycle, at least in solution, is a low-energy process and fast on the NMR time scale. Such fluxional behavior is consistent with the NMR spectrum of the complex recorded at 298 K, which shows no apparent splitting of the polycycle methylene signals.

**b. Formation of a 2:1 Complex.** Mass spectra (FAB mode) were recorded for matrix samples of ADIQ•2PF<sub>6</sub> containing varying amounts of CE(10). As shown in Figure 7, peak clusters occurring at  $m/z = 1039.5 \{ \text{CE}(10) \cdot \text{ADIQ} \cdot \text{PF}_6 \}^+$  and  $895 \{ \text{CE}(10) \cdot \text{ADIQ} \}^{2+}$  are consistent with 1:1 complexation. This is clear support for the NMR and fluorescence binding studies. However, at high mole fractions of CE(10) there are small clusters that endorse a CE(10):ADIQ•2PF<sub>6</sub> ratio of 2:1 ( $m/z = 1576$  and  $1431$ ) (Figure 7). Allowing for the NMR findings, we can surmise that the 2:1 complex exists as a [3]pseudorotaxane (Figure 6). There is in fact a literature precedent for a

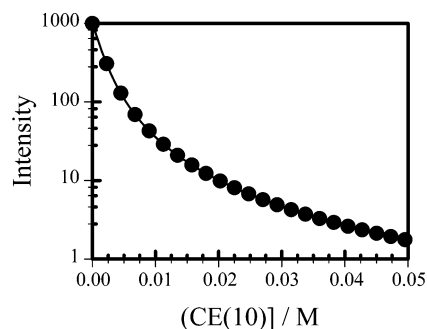


**Figure 8.** Effect of added CE(10) on fluorescence quantum yield measured for ADIQ•2PF<sub>6</sub> in deoxygenated acetonitrile containing background electrolyte. The solid line drawn through the data points corresponds to a fit to successive 1:1 and 1:2 complexation with  $K_1 = 510 \text{ dm}^3 \text{ mol}^{-1}$  and  $K_2 = 430 \text{ dm}^3 \text{ mol}^{-1}$ .

related [3]pseudorotaxane formed between DAP•2PF<sub>6</sub> and a smaller crown ether.<sup>40</sup>

The fluorescence titration data were subsequently reanalyzed over a much wider concentration range and considered in terms of both 1:1 and 2:1 complexation (Figure 8). In acetonitrile at 20 °C, this analysis gave successive binding constants of  $K_1 = 510 \text{ dm}^3 \text{ mol}^{-1}$  and  $K_2 = 430 \text{ dm}^3 \text{ mol}^{-1}$ . It is notable that the fit at high CE(10) concentrations is markedly improved by allowing for formation of the 2:1 complex. The ratio of binding constants indicates the absence of significant cooperativity but is consistent with a simple statistical model. Once again computer molecular modeling studies were made with the reactants dispersed in a matrix of 96 acetonitrile molecules and starting with a fixed stoichiometry of 1:2 (ADIQ•2PF<sub>6</sub>:CE(10)). A number of starting conformations were tried, and the initial positions of the two PF<sub>6</sub><sup>-</sup> anions were also varied. The energy-minimized structure (Figure 6) clearly illustrates the docking of two CE(10) macrocycles to the N-methylated aza ends of the polyaromatic rod. As observed for the 1:1 complex, both crown ethers distort so as to permit preferential binding of five oxygen atoms to the two ends of the ADIQ<sup>2+</sup> subunit at any given time.

**c. Photophysics of the Conjugate.** The high fluorescence yield shown by ADIQ•2PF<sub>6</sub> made it difficult to carry out detailed laser spectroscopic studies on the complexes, especially the 1:1 complex, since free ADIQ•2PF<sub>6</sub> could not be avoided. To maximize complexation, studies were made in acetonitrile solution<sup>41</sup> with a 50-fold excess of CE(10). Under these conditions, approximately 90% of ADIQ•2PF<sub>6</sub> should be complexed, with the 2:1 complex (67%) predominating. Of the available excitation wavelengths, 554 nm turned out to be the most appropriate since it allowed selective excitation into the charge-transfer absorption band. Although the molar absorption coefficient of the complex is small at 554 nm, and high concentrations of complex led to precipitation, it was possible to identify suitable experimental conditions under which to study the photophysics of the charge-transfer complex.

Thus, excitation of the complex in butyronitrile at room temperature with a subpicosecond laser pulse at 554 nm resulted in the rapid appearance of a sharp absorption band centered around 650 nm (Figure 9a). This band is characteristic of the ADIQ  $\pi$ -radical cation (ADIQ<sup>•+</sup>), as shown previously by pulse radiolysis studies.<sup>28</sup> The signal grows with a time constant of ca. 3 ps before decaying via first-order kinetics with a lifetime of ca. 25 ps (Figure 9b). Formation of ADIQ<sup>•+</sup> on this time scale must arise from electron transfer within the charge-transfer complex. As such, the 25-ps lifetime may be attributed to charge recombination within the initially formed radical ion pair (RIP).

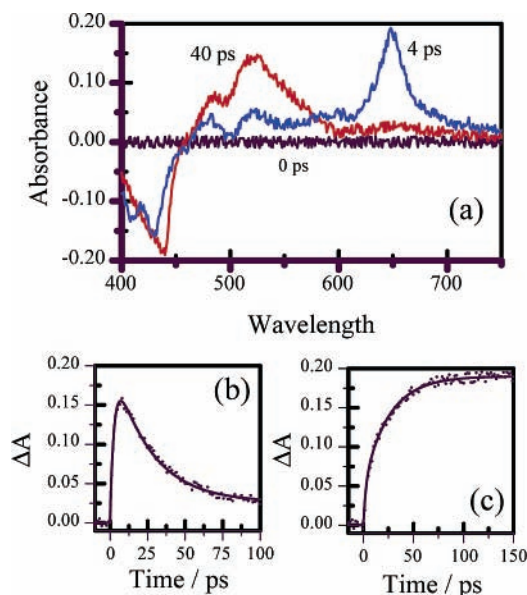


**Figure 9.** (a) Transient absorption spectra recorded after excitation of the complex with a subpicosecond laser pulse at 554 nm. (b) Kinetic profile recorded at 650 nm. (c) Kinetic profile recorded at 520 nm.

The high rate found for this process essentially precludes diffusive separation of the RIP into solvated radical ions.<sup>42</sup> Indeed, the signal assigned to  $\text{ADIQ}\cdot^+$  disappears completely within ca. 100 ps.

Examination of the spectral profile in the region around 520 nm shows that rapid charge recombination within the RIP results in formation of the triplet excited state localized on  $\text{ADIQ}\cdot 2\text{PF}_6$  (Figure 9c). Comparison with the uncomplexed system indicates that the quantum yield for triplet formation increases from 0.07 to 0.85 upon complexation (Figure 3b).<sup>43</sup> There is also a 1000-fold increase in the rate of triplet population for the complex relative to isolated  $\text{ADIQ}\cdot 2\text{PF}_6$ . Triplet formation competes effectively with charge recombination to reform the ground state, despite the need for spin conversion. Presumably this competition is a consequence of the energy gap law<sup>44</sup> since triplet formation involves dissipation of only ca. 0.9 eV compared to ca. 2.3 eV involved in restoration of the ground state. The triplet state formed in this manner shows no sign of decay over 10 ns and presumably has a lifetime ( $\tau_T = 470 \mu\text{s}$ ) similar to that found for isolated  $\text{ADIQ}\cdot 2\text{PF}_6$  in deoxygenated solution.

The net result of illumination into the charge-transfer complex, therefore, is greatly enhanced intersystem crossing to the triplet manifold. Clearly, this is a consequence of the low triplet energy associated with  $\text{ADIQ}\cdot 2\text{PF}_6$ . It is assumed that both 1:1 and 2:1 complexes show similar behavior. There is no observable separation of the radical ion pair into solvent-separated ions, despite the expected Coulombic repulsion and the apparent loose docking between the reactants. This latter finding is in agreement with the photophysics of related conjugates.<sup>13</sup>

**Acknowledgment.** This work was supported by the Universities of Glasgow and Newcastle, the Nuffield Foundation (A.C.B.), the Royal Society of London (A.H.) and the Engineering & Physical Sciences Research Council (C.S.). A Royal Society of Chemistry JWT Jones Travel Fellowship (A.C.B.) is also gratefully acknowledged.

## References and Notes

- (1) (a) Fabbrizzi, L.; Foti, F.; Licchelli, M.; Maccarini, P. M.; Sacchi, D.; Zema, M. *Chem. Eur. J.* **2002**, *8*, 4965. (b) Ball, P. *Nanotechnology* **2002**, *13*, R15. (c) Colasson, B. X.; Dietrich-Buchecker, C.; Jimenez-Molero, M. C.; Sauvage, J.-P. *J. Phys. Org. Chem.* **2002**, *15*, 476. (d) Amendola, V.; Fabbrizzi, L.; Mangano, C.; Miller, H.; Pallavicini, P.; Perotti, A.; Taglietti, A. *Angew. Chem., Int. Ed.* **2002**, *41*, 2553. (e) Kim, K. *Chem. Soc. Rev.* **2002**, *31*, 96. (f) Day, A. I.; Blanch, R. J.; Arnold, A. P.; Lorenzo, S.; Lewis, G. R.; Dance, I. *Angew. Chem., Int. Ed.* **2002**, *41*, 275. (g) Raehm, L.; Sauvage, J.-P. *Struct. Bond.* **2001**, *99*, 55. (h) Harada, A. *Acc. Chem. Res.* **2001**, *34*, 456. (i) Balzani, V.; Credi, A.; Raymo, F. M.; Stoddart, J. F. *Angew. Chem., Int. Ed.* **2000**, *39*, 3349. (j) de Silva, A. P.; Gunaratne, H. Q. N.; Gunnlaugsson, T.; Huxley, A. J. M.; McCoy, C. P.; Rademacher, J. T.; Rice, T. E. *Chem. Rev.* **1997**, *97*, 1515. (k) Ward, M. D. *Chem. Ind. (London)* **1997**, 640. (l) Kaifer, A. E. *Acc. Chem. Res.* **1999**, *32*, 42. (2) Benniston, A. C. *Chem. Soc. Rev.* **1996**, *25*, 427. (3) (a) Leigh, D. A.; Murphy, A. *Chem. Ind. (London)* **1999**, 178. (b) Benniston, A. C.; Mackie, P. R. *Handbook of Nanostructured Materials and Nanotechnology*, concise ed.; Nalwa, H. S., Ed.; Academic Press: New York, 2001; p 693. (4) (a) Collin, J.-P.; Laemmel, A. C.; Sauvage, J.-P. *New J. Chem.* **2001**, *25*, 22. (b) Wurlpel, G. W. H.; Brouwer, A. M.; van Stokkum, I. H. M.; Farran, A.; Leigh, D. A. *J. Am. Chem. Soc.* **2001**, *123*, 11327. (c) Fujimoto, T.; Nakamura, A.; Inoue, Y.; Sakata, Y.; Kaneda, T. *Tetrahedron Lett.* **2001**, *42*, 7987. (d) Balzani, V.; Credi, A.; Marchioni, F.; Stoddart, J. F. *Chem. Commun.* **2001**, 1860. (e) Ashton, P. R.; Ballardini, R.; Balzani, V.; Credi, A.; Dress, K. R.; Ishow, E.; Kleverlaan, C. J.; Kocian, O.; Preece, J. A.; Spencer, N.; Stoddart, J. F.; Venturi, M.; Wenger, S. *Chem. Eur. J.* **2000**, *6*, 3558. (f) Willner, I.; Pardo-Yissar, V.; Katz, E.; Ranjit, K. T. *J. Electroanal. Chem.* **2001**, *497*, 172. (g) Benniston, A. C.; Harriman, A.; Lynch, V. M. *J. Am. Chem. Soc.* **1995**, *117*, 5279. (5) (a) Collin, J.-P.; Dietrich-Buchecker, C.; Gavina, P.; Jimenez-Molero, M. C.; Sauvage, J.-P. *Acc. Chem. Res.* **2001**, *34*, 477. (b) Ballardini, R.; Balzani, V.; Di Fabio, A.; Gandolfi, M. T.; Becher, J.; Lau, J.; Nielsen, M. B.; Stoddart, J. F. *New J. Chem.* **2001**, *25*, 293. (c) Balzani, V.; Credi, A.; Matternsteig, G.; Matthews, O. A.; Raymo, F. M.; Stoddart, J. F.; Venturi, M.; White, A. J. P.; Williams, D. J. *J. Org. Chem.* **2000**, *65*, 1924. (d) Bidan, G.; Billon, M.; Diisia-Blohorn, B.; Kern, J.-M.; Raehm, L.; Sauvage, J.-P. *New J. Chem.* **1998**, *22*, 1139. (6) (a) Gibson, H. W.; Yamaguchi, N.; Hamilton, L.; Jones, J. W. *J. Am. Chem. Soc.* **2002**, *124*, 4653. (b) Wang, L. Y.; Xi, H. T.; Sun, X. Q.; Pan, Y.; Hu, H. W. *Chem. J. Chin. Univ.-Chin.* **2001**, *22*, 143. (c) Balzani, V.; Credi, A.; Matternsteig, G.; Matthews, O. A.; Raymo, F. M.; Stoddart, J. F.; Venturi, M.; White, A. J. P.; Williams, D. J. *J. Org. Chem.* **2000**, *65*, 1924. (7) (a) Sauvage, J.-P. *Acc. Chem. Res.* **1998**, *31*, 611. (b) Jimenez, M. C.; Dietrich-Buchecker, C.; Sauvage, J.-P. *Angew. Chem., Int. Ed.* **2000**, *39*, 3284. (c) Jimenez-Molero, M. C.; Dietrich-Buchecker, C.; Sauvage, J.-P. *Chem. Eur. J.* **2002**, *8*, 1456. (8) (a) Balzani, V.; Credi, A.; Marchioni, F.; Stoddart, J. F. *Chem. Commun.* **2001**, 1860. (b) Yamaguchi, I.; Osakada, K.; Yamamoto, T. *Chem. Commun.* **2000**, 1335. (9) Benniston, A. C.; Harriman, A.; Philp, D.; Stoddart, J. F. *J. Am. Chem. Soc.* **1993**, *115*, 5298. (10) Colquhoun, H. M.; Goodings, E. P.; Maud, J. M.; Stoddart, J. F.; Williams, D. J.; Wolstenholme, J. B. *J. Chem. Soc., Perkin Trans. 2* **1985**, 607. (11) Benniston, A. C.; Harriman, A. In *NATO Advanced Workshop on Physical Supramolecular Chemistry*; Kaifer, A. E., Echegoyen, L., Eds.; 1996; p 179. (12) Ballardini, R.; Balzani, V.; Gandolfi, M. T.; Prodi, L.; Venturi, M.; Philp, D.; Ricketts, H. G.; Stoddart, J. F. *Angew. Chem., Int. Ed. Engl.* **1993**, *32*, 1301. (13) Benniston, A. C.; Harriman, A.; Yufit, D. S. *Angew. Chem., Int. Ed. Engl.* **1997**, *36*, 2356. (14) Balzani, V.; Gomez-Lopez, M.; Stoddart, J. F. *Acc. Chem. Res.* **1998**, *31*, 405. (15) (a) Wasielewski, M. R.; Minsek, D. W.; Niemczyk, M. P.; Svec, W. A.; Yang, N. C. *J. Am. Chem. Soc.* **1990**, *112*, 2823. (b) Brun, A. M.; Harriman, A.; Tsuboi, Y.; Okada, T.; Mataga, N. *J. Chem. Soc., Faraday Trans.* **1995**, *91*, 4047. (c) van Dijk, S. I.; Wiering, P. G.; Groen, C. P.; Brouwer, A. M.; Verhoeven, J. W.; Schuddeboom, W.; Warman, J. M. *J. Chem. Soc., Faraday Trans.* **1995**, *91*, 2107. (d) Khundkar, L. R.; Stiegman, A. E.; Perry, J. W. *J. Phys. Chem.* **1990**, *94*, 1224. (e) Biswas, M.; Nguyen, P.; Marder, T. B.; Khundkar, L. R. *J. Phys. Chem. A* **1997**, *101*, 1689. (16) Anelli, P. L.; Ashton, P. R.; Ballardini, R.; Balzani, V.; Delgado, M.; Gandolfi, M. T.; Goodnow, T. T.; Kaifer, A. E.; Philp, D.; Pietraszkiewicz, M.; Prodi, L.; Reddington, M. V.; Slawin, A. M. Z.; Spencer, N.; Stoddart, J. F.; Vicent, C.; Williams, D. J. *J. Am. Chem. Soc.* **1992**, *114*, 193. (17) Hüning, S.; Grosse, J.; Lier, E. F.; Quast, H. *Leibigs Ann. Chem.* **1973**, 339. (18) Hynes, M. J. *J. Chem. Soc., Dalton Trans.* **1993**, 311. (19) Atherton, S. J.; Harriman, A. *J. Am. Chem. Soc.* **1993**, *115*, 1816. (20) Davila, J.; Harriman, A. *Photochem. Photobiol.* **1990**, *51*, 9. (21) Pekkarinen, L.; Linschitz, H. *J. Am. Chem. Soc.* **1960**, *82*, 2407.

- (22) Hurley, J. K.; Sinai, N.; Linchitz, H. *Photochem. Photobiol.* **1983**, *38*, 9.
- (23) © Wavefunction Inc.
- (24) The absorption spectrum was converted from nm to  $\text{cm}^{-1}$  and fitted using PEAKFIT to a single Gaussian profile. The peak maximum and half-width were taken from the analysis.
- (25) (a) Watson, D. F.; Bocarsly, A. B. *Coord. Chem. Rev.* **2001**, *211*, 177. (b) Walters, K. A.; Trouillet, L.; Guillerez, S.; Schanze, K. S. *Inorg. Chem.* **2000**, *39*, 5496. (c) Arnold, B. R.; Zaini, R.; Euler, A. *Spectrosc. Lett.* **2000**, *33*, 595. (d) Proppe, B.; Merchan, M.; Serrano-Andres, L. *J. Phys. Chem. A* **2000**, *104*, 1608. (e) Cacelli, I.; Ferretti, A. *J. Phys. Chem. A* **1999**, *103*, 4438.
- (26) (a) Waters, M. L. *Curr. Opin. Chem. Biol.* **2002**, *6*, 736. (b) Tsuzuki, S.; Honda, K.; Azumi, R. *J. Am. Chem. Soc.* **2002**, *124*, 12200. (c) Mecdr, O.; Ferreira, J. A.; Nascimento, S. M.; Burrows, H. D.; Miguel, M. D. *J. Chem. Soc., Faraday Trans.* **1995**, *91*, 3913. (d) So, Y. H.; Zaleski, J. M.; Murlick, C.; Ellaboudy, A. *Macromolecules* **1996**, *29*, 2783.
- (27) Other forms of bonding are likely involved in complexation. Most notable are electrostatic interactions and ion-dipole forces. It is considered unlikely that the main stabilization of the complex arises from  $\pi$ -stacking between the polycycle and the benzene rings of the crown ether.
- (28) Brun, A. M.; Harriman, A. *J. Am. Chem. Soc.* **1991**, *113*, 8153.
- (29) Marcus, R. A.; Sutin, N. *Biochim. Biophys. Acta* **1985**, *811*, 265.
- (30) Brun, A. M.; Harriman, A.; Hubig, S. M. *J. Phys. Chem.* **1992**, *96*, 254.
- (31) (a) Bixon, M.; Jortner, J.; Cortes, J.; Heitele, H.; Michel-Beyerle, M. E. *J. Phys. Chem.* **1994**, *98*, 7289. (b) Cortes, J.; Heitele, H.; Jortner, J. *J. Phys. Chem.* **1994**, *98*, 2527.
- (32) Strickler, S. J.; Berg, R. A. *J. Chem. Phys.* **1962**, *37*, 814.
- (33) McGlynn, S. P.; Azumi, T.; Kinoshita, M. *Molecular Spectroscopy of the Triplet State*; Prentice-Hall: Englewood Cliffs, NJ, 1969.
- (34) (a) Nemzek, T. L.; Ware, W. R. *J. Chem. Phys.* **1975**, *62*, 477. (b) Armspach, D.; Matt, D.; Harriman, A. *Eur. J. Inorg. Chem.* **2000**, 1147.
- (35) (a) Binding constants were measured by fluorescence spectroscopy at relatively low concentrations of CE(10) in a range of solvents of different Gutmann donor number. The derived stability constants (given in units of  $\text{dm}^3 \text{mol}^{-1}$ ) are as follows (with the donor number given in parentheses): nitromethane (2.7) 1950; benzonitrile (11.9) 900; acetonitrile (14.1) 500; propylene carbonate (15.1) 480; propionitrile (16.1) 440; butyronitrile (16.6) 420; acetone (17) 725; formamide (24) 280; *N,N*-dimethylformamide (26.6) 210; *N*-methylformamide (27) 200; dimethyl sulfoxide (29.8) 150. (b) Mayer, U. *Pure Appl. Chem.* **1979**, *51*, 1697.
- (36) Marquis, D.; Grieving, H.; Desvergne, J.-P.; Lahrahar, N.; Marsau, P. *Liebigs Ann. Org. Bioorg. Chem.* **1997**, *1*, 97.
- (37) (a) Lehn, J.-M. *Supramolecular Chemistry—Concepts and Perspectives*; VCH: Weinheim, 1995. (b) Balzani, V.; Venturi, M.; Credi, A. *Molecular Devices and Machines: A Journey into the Nanoworld*; Wiley-VCH: Weinheim, 2003.
- (38) Lamsa, M.; Huuskonen, J.; Rissanen, K.; Pursiainen, J. *Chem. Eur. J.* **1998**, *4*, 84.
- (39) Ashton, P. R.; Ballardini, R.; Balzani, V.; Credi, A.; Gandolfi, M. T.; Menzer, S.; Pérez-García, L.; Prodi, L.; Stoddart, J. F.; Venturi, M.; White, A. J. P.; Williams, D. J. *J. Am. Chem. Soc.* **1995**, *117*, 11171.
- (40) Ashton, P. R.; Langford, S. J.; Spencer, N.; Stoddart, J. F.; White, A. J. P.; Williams, D. J. *Chem. Commun.* **1996**, 1387.
- (41) The solution also contained ammonium hexafluorophosphate ( $0.1 \text{ mol dm}^{-3}$ ) as background electrolyte. Measurements were made after deoxygenation by purging with  $\text{N}_2$ , but it was found that the presence of  $\text{O}_2$  had no effect on the kinetics.
- (42) The high yield of the triplet state formed during charge recombination makes it difficult to obtain an accurate measurement of the yield of separated radical ions. Monitoring at 650 nm, the absorption maximum for  $\text{ADIQ}^{*+}$ , we estimate that less than 15% of the initially formed RIP dissociates into solvent-separated radical ions. This is a generous estimate since we do not see any separated species.
- (43) In making this calculation, it is assumed that the differential absorption coefficient for the triplet state remains unaffected by complexation.
- (44) Englman, R.; Jortner, J. *Mol. Phys.* **1970**, *18*, 145.